Current Biology, Vol. 12, 253–265, February 19, 2002, ©2002 Elsevier Science Ltd. All rights reserved. PII S0960-9822(02)00683-8

Identification of a Novel Ras-Regulated Proapoptotic Pathway

Andrei Khokhlatchev,[1,2,3] Shahrooz Rabizadeh,[2,4] Ramnik Xavier,[2,3] Maria Nedwidek,[1,2,3] Tao Chen,[2] Xian-feng Zhang,[2] Brian Seed,[2,4] and Joseph Avruch[1,2,3,5]
[1]Diabetes Unit and Medical Services
[2]Department of Molecular Biology
Massachusetts General Hospital
[3]Department of Medicine
[4]Department of Genetics
Harvard Medical School
Boston, Massachusetts 02114

Summary

Background: The Ras-GTPase controls cell fate decisions through the binding of an array of effector molecules, such as Raf and PI 3-kinase, in a GTP-dependent manner. NORE1, a noncatalytic polypeptide, binds specifically to Ras-GTP and to several other Ras-like GTPases. NORE is homologous to the putative tumor suppressor RASSF1 and to the *Caenorhabditis elegans* polypeptide T24F1.3.

Results: We find that all three NORE-related polypeptides bind selectively to the proapoptotic protein kinase MST1, a member of the Group II GC kinases. Endogenous NORE and MST1 occur in a constitutive complex in vivo that associates with endogenous Ras after serum stimulation. Targeting recombinant MST1 to the membrane, either through NORE or myristoylation, augments the apoptotic efficacy of MST1. Overexpression of constitutively active Ki-RasG12V promotes apoptosis in a variety of cell lines; Ha-RasG12V is a much less potent proapoptotic agent; however, a Ha-RasG12V effector loop mutant (E37G) that binds NORE, but not Raf or PI 3-kinase, exhibits proapoptotic efficacy approaching that of Ki-RasG12V. The apoptotic action of both Ki-RasG12V and Ha-RasG12V, E37G is suppressed by overexpression of the MST1 carboxy-terminal noncatalytic segment or by the NORE segment that binds MST1.

Conclusions: MST1 is a phylogenetically conserved partner of the NORE/RASSF polypeptide family, and the NORE-MST1 complex is a novel Ras effector unit that mediates the apoptotic effect of Ki-RasG12V.

Background

Ras is a small GTPase imbedded on the inner surface of the plasma membrane whose primary function is to relay proliferative and developmental signals downstream of cell surface receptors, especially, but not exclusively, receptor tyrosine kinases [1]. Ras signaling is activated on binding GTP, which results in the reconfiguration of two epitopes on the cytoplasmic face of the Ras polypeptide, thereby creating binding sites for Ras "effector" proteins [2]. The first Ras effectors to be identified were the kinases of the Raf subfamily, which are activated consequent to binding Ras-GTP in vivo and in turn activate the classic MAPK pathway [3]. It is now well recognized that Ras utilizes effectors in addition to the Raf kinases. Among the earliest evidence was the observation that, although active mutants of both Ras and Raf can transform cell lines of fibroblastic origin, spontaneously occurring active Ras mutants are mostly found in human tumors of epithelial origin [4]. Whereas active Ras alone can transform epithelial cell lines, active Raf mutants do not [5]. Certain Ras effector loop mutants that have lost the ability to bind and activate Raf and to transform fibroblasts nevertheless can collaborate with each other, or with weakly active, nontransforming Raf mutants, to achieve cellular transformation [6, 7]. Regarding cellular, wild-type Ras, it is known that, although at least two peaks of increased Ras-GTP charging occur during G1 progression, only the earlier peak is accompanied by an increase in MAPK activity; the relevant effector in mid-late G1 is not known [8]. Direct support for the existence of multiple Ras effectors comes from the identification of proteins, other than the Raf kinases, that can bind to Ras in a GTP-dependent manner, including, e.g., the protein kinases MEKK1 and PKCζ [1]. Whereas the role of these protein kinases in Ras action is unknown, considerable evidence indicates that the catalytic subunits of the Type 1 PI 3-kinases are bona fide Ras effectors. These p110 polypeptides each bind specifically to Ras-GTP through a structurally conserved domain; mutation within this domain that interrupts Ras-GTP binding increases basal PI 3-kinase activity and significantly reduces RTK activation of PI 3-kinase activity in vivo [9]. A third class of probable Ras effectors is the family of guanylnucleotide exchange factors active on the Ral A GTPase (Ral-GDS, Rgl, Rlf). These polypeptides also bind selectively to Ras-GTP through a conserved noncatalytic domain [10]. In addition, several noncatalytic polypeptides have been isolated by their ability to bind specifically to Ras-GTP, including AF-6 [11], Rin1 [12], and NORE [13]; the latter is the subject of this report.

Ras was first identified in mutant, active form as a retroviral-transforming agent. Moreover, mutations conferring constitutive Ras activation are found in nearly 30% of all human tumors [4]. Although active Ras mutants are able to transform nearly all immortalized cell lines, they are usually unable to transform normal primary cells [14], except in the presence of a cooperating oncogene [15–17] or in association with the loss of certain tumor suppressor genes [18, 19]. Introduction of constitutively active Ras into primary cells generally results in cell cycle arrest mediated by increased levels of a variety of cyclin-dependent kinase inhibitors, or in apoptosis [19–21]. Downregulation of the pathways mediating cell cycle arrest and/or apoptosis is probably crucial to the expression of Ras-induced oncogenesis. The mechanism by which Ras promotes G1 cell cycle

[5]Correspondence: avruch@helix.mgh.harvard.edu

arrest has received considerable attention, whereas the mechanism by which constitutively active Ras promotes apoptosis has been much less extensively explored. Oncogenic Ras strongly stimulates the activation of p53 through the induction of $p14^{ARF}$, which neutralizes the p53 inhibitor MDM2 [22, 23]. The ability of active alleles of Ras to cause apoptosis of primary mouse embryo fibroblasts (MEF) is greatly diminished by homozygous deletion of the gene encoding p53 [24]. The existence of additional p53-independent pathways for Ras-induced apoptosis is indicated by the ability of RasG12V to promote apoptosis if the Ras-induced increase in NFκb activity is suppressed [25, 26] either in $p53^{-/-}$ mouse embryo fibroblasts or in $53^{+/+}$ NIH3T3 cells expressing $p53^{v135}$, a temperature-sensitive dominant inhibitor of p53. Phorbol ester-induced downregulation of PKCs induces apoptosis in Ras-transformed cells [27]. Thus, as is true for Ras-induced proliferation, multiple pathways exist for Ras induction of apoptosis. In the present report, we identify a novel pathway by which active Ki-Ras initiates apoptosis through the direct recruitment of its putative effector NORE, which is stably associated with the proapoptotic, Ste20-related protein kinase MST1.

Results

The putative Ras effector NORE is a 413 amino acid noncatalytic polypeptide that contains several proline-rich motifs between amino acids 17 and 108, a central C1 zinc finger motif (aa 118–165), and a Ras association (RA) domain in its carboxy-terminal segment (aa 267–358) [13]. Although we showed previously [13] that NORE binds directly to Ras-GTP and is recruited to cRas in vivo in response to EGF, the biologic roles and biochemical functions of NORE are as yet unknown

NORE is most closely related in structure to a family of human polypeptides encoded by the *RASSF1* gene on Chr3p21 [28, 29]. Five splice variants of *RASSF1* have been reported ranging from aa 189 to aa 344. The three longest *RASSF1* isoforms, A, D, and E (340, 344, and 344 amino acids, respectively), each contain a central C1 zinc finger upstream of an RA domain and are approximately 50% identical (75% similar) in amino acid sequence to the carboxy-terminal 300 amino acids of NORE (Figure 1A). The 270 amino acid RASSF1C isoform is identical over its C-terminal 221 amino acids to the longer RASSF1 polypeptides but contains a unique 49 amino acid N-terminal segment; RASSF1C thus lacks the C1 zinc finger motif but contains the RA domain. The *C. elegans* gene product T24F1.3 is a 615 amino acid polypeptide containing a unique amino-terminal segment, a central C1 zinc finger (aa 165–214), a putative RA domain (aa 396–495), and a C-terminal extension of 65 amino acids relative to NORE and RASSF1A; the carboxy-terminal 300 amino acids of the latter two polypeptides are each about 40% identical (70% similar) in amino acid sequence to the central segment of T24F1.3 (Figure 1A), suggesting that T24F1.3, which contains the C1 and RA domains, is a common precursor to these two mammalian polypeptides.

The chromosomal segment encompassing the *RASSF1* gene (3p21.3) exhibits loss of heterozygosity in 90% of small cell lung cancers (SCLC) and in 50%–80% of non-small cell lung cancers (NSCLC) [28, 29], breast cancers [30, 31], clear cell renal cancers [32], and several other solid tumors. Moreover, the expression of the longer isoforms, specifically RASSF1A, is selectively extinguished in all SCLC-derived cell lines examined and in a variety of other tumor-derived cell lines, through mutation, or more frequently, methylation of the RASSF1A promoter [29–32]. Selective reexpression of the RASSF1A polypeptide suppresses the growth in vitro and the tumorgenicity in vivo of these cell lines [29–31].

NORE, RASSF1, and T24F1.3 Each Bind MST1

The tumor suppressor function attributed to RASSF1A together with the presence of an RA domain homologous to that in NORE raised the possibility that these polypeptides might participate in Ras-induced apoptosis. Surprisingly, in comparison to NORE, neither RASSF1 nor the *C. elegans* polypeptide T24F1.3 exhibited any significant ability to bind directly to RasG12V or several related GTPases, as determined quantitatively in a yeast two-hybrid assay, by cotransfection in mammalian cells [33] or by binding in vitro (see below). Thus, while RASSF1 is unlikely to be a direct mediator of Ras function, the similarity between NORE, RASSF1A, and the central domain of T24F1.3A suggests that some evolutionarily conserved function was shared by these proteins. We therefore employed yeast two-hybrid expression cloning in an effort to identify proteins that bound to all three NORE-related polypeptides. In screening cDNA libraries with either NORE or RASSF1A, we found several candidates that interacted with both baits; however, only one also bound to T24F1.3, a murine cDNA encoding the Ste20-related protein kinase MST1 (Figure 1A). The prior demonstration that MST1 can act as a proapoptotic agent impelled us to examine further this evolutionarily conserved interaction. We elected to focus on the NORE- MST1 interaction, in view of the clear-cut relationship between Ras and NORE.

Murine MST1 is a 487 amino acid polypeptide that migrates near 60 kDa on SDS PAGE [34, 35]. MST1 contains an amino-terminal kinase catalytic domain (aa 30–281; 88% identical to MST2) and a noncatalytic carboxy-terminal tail; its overall architecture and catalytic domain sequence place it as a Group II GC kinase [36]. Little is known concerning the physiologic regulation of MST1. As for the targets downstream of MST1, no effect on ERK 1/2 activity has been observed, and activation of coexpressed SAPK/JNK or p38 has been observed in some reports [37], but not others [34, 38]. In contrast, overexpression of MST1 or MST1 (1–330) (but not kinase-inactive MST1) results in apoptosis in several cell backgrounds.

FLAG-tagged versions of NORE, RASSF1A, RASSF1C, and T24F1.3 each bind specifically with GST-MST1 during transient expression in COS-7 cells (Figure 1A). The binding site for MST1 is located on the carboxy-terminal portions of NORE (Figures 1A and 1B) and RASSF1A (Figure 1A). The site on NORE responsible for binding MST1 was mapped more closely and was shown to be the carboxy-terminal segment, distal to the RA domain; thus, fusion of the NORE segment (358–413)

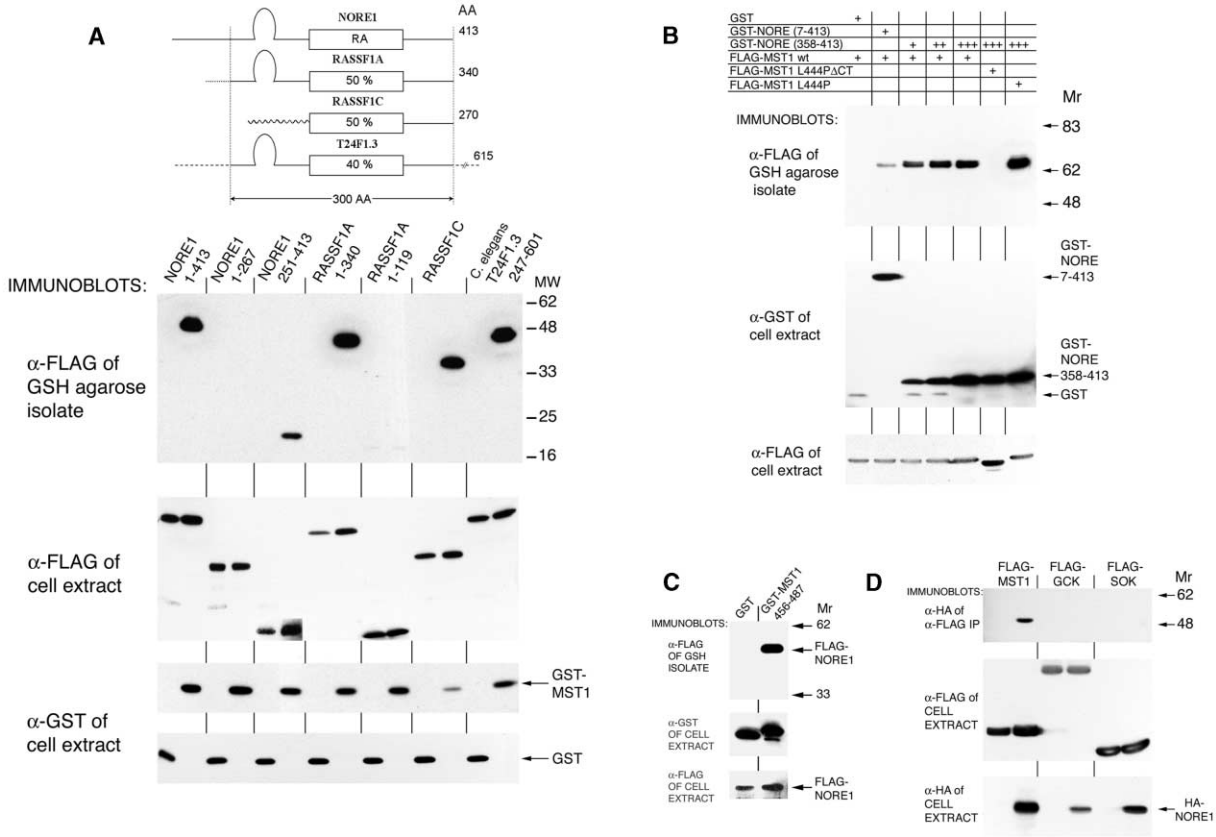

Figure 1. NORE1 and Its Homologs RASSF1 and T24F1.3 Bind MST1

(A) Binding FLAG-NORE1 homologs by GST-MST1. COS-7 cells were transfected with either a vector (pEBG) endcoding GST or a GST-MST1 fusion protein, together with FLAG-tagged NORE1, NORE (1–267), NORE (251–413), or the NORE1 homologs RASSF1A (full length, 1–340) RASSF1A (1–119), RASSF1C, or a fragment of the *C. elegans* polypeptide T24F1.3 (247–601). GST and the various GST fusion proteins were purified using GSH-agarose and analyzed by immunoblotting after SDS PAGE. Upper panel: proteins retained on GSH beads were probed with anti-FLAG (M2 monoclonal, Sigma) antibody. Second panel: cell extracts probed with anti-FLAG antibody. Third and fourth panels: cell extracts probed with anti-GST antibody. Mr, molecular weight markers, kDa. The cartoon indicates the domain features of the NORE-related polypeptides and identifies the 300 amino acid segment of homology.

(B) MST1 binds NORE carboxy-terminal to the NORE-RA domain. HEK293 cells were transfected with expression vectors encoding GST, GST-NORE (7–413), or GST-NORE (358–413), the latter at increasing levels as compared with GST-NORE (7–413), together with FLAG-tagged wild-type MST1, or MST1 Leu444Pro (L444P) or MST1 (L444P), with a frameshift after amino acid 449 that replaces the carboxy-terminal 38 amino acids of the MST1 with an unrelated 8 amino acid segment (L444PΔCT). GST and GST fusion proteins were isolated from cell extracts by adsorption to GSH-agarose and analyzed by immunoblotting after SDS PAGE. Upper panel: proteins retained on GSH beads were probed with anti-FLAG antibody. Middle panel: cell extracts probed with anti-GST antibody. Lower panel: cell extracts probed with anti-FLAG antibody.

(C) The MST1 carboxy-terminal 32 amino acids are sufficient to bind FLAG-NORE1. COS-7 cells were transfected with expression vectors encoding GST or GST-MST1 (456–487) together with FLAG-NORE1. GST and GST-MST1 (456–487) were isolated on GSH-agarose and were analyzed by immunoblotting after SDS PAGE. Upper panel: proteins retained on GSH-agarose beads probed with anti-FLAG antibody. Middle panel: cell extracts probed with anti-GST antibody. Bottom panel: cell extracts probed with anti-FLAG antibody.

(D) NORE1 binds MST 1, but not related kinases. HEK293 cells were transfected with expression vectors encoding HA-NORE 1 and FLAG-tagged MST1, GCK, or SOK as indicated. FLAG-tagged proteins were immunoprecipitated with anti-FLAG M2-agarose, eluted with the excess of the FLAG pepetide. The eluates were analyzed by immunoblotting after SDS PAGE. Upper panel: proteins immunoprecipitated by FLAG-agarose probed with 12CA5 antibody. Middle panel: cell extracts probed with anti-FLAG antibody. Lower panel: cell extracts probed with anti-HA antibody.

onto GST is sufficient to confer the binding of full-length MST1 (Figure 1B). The MST1 segment responsible for binding NORE is at the MST1 C terminus. Deletion of MST1 amino acids 449–487 abolishes binding to GST-NORE (358–413) (Figure 1B), whereas fusion of the MST1 C-terminal 33 amino acids (456–487) to GST is sufficient to enable the specific binding of FLAG-NORE (Figure 1C). Moreover, MST1 dimerization is not required for association to NORE, as the dimerization-deficient MST1 (L444P) mutant exhibits unimpaired binding to GST-NORE (358–413) (Figure 1B).

The specificity of NORE binding to MST1 was evaluated by the examination of NORE binding to other representative GC kinase homologs [36]; thus, GCK or SOK1 do not bind to NORE (Figure 1D). NORE does bind MST2 (data not shown); we have not examined MST3.

NORE and MST1 Exist as a Complex In Vivo

We next examined whether endogenous NORE and MST1 exist in a complex in vivo. As shown previously, although KB cell extracts exhibit two major bands (at 46 kDa and 55 kDa) reactive on immunoblot with our

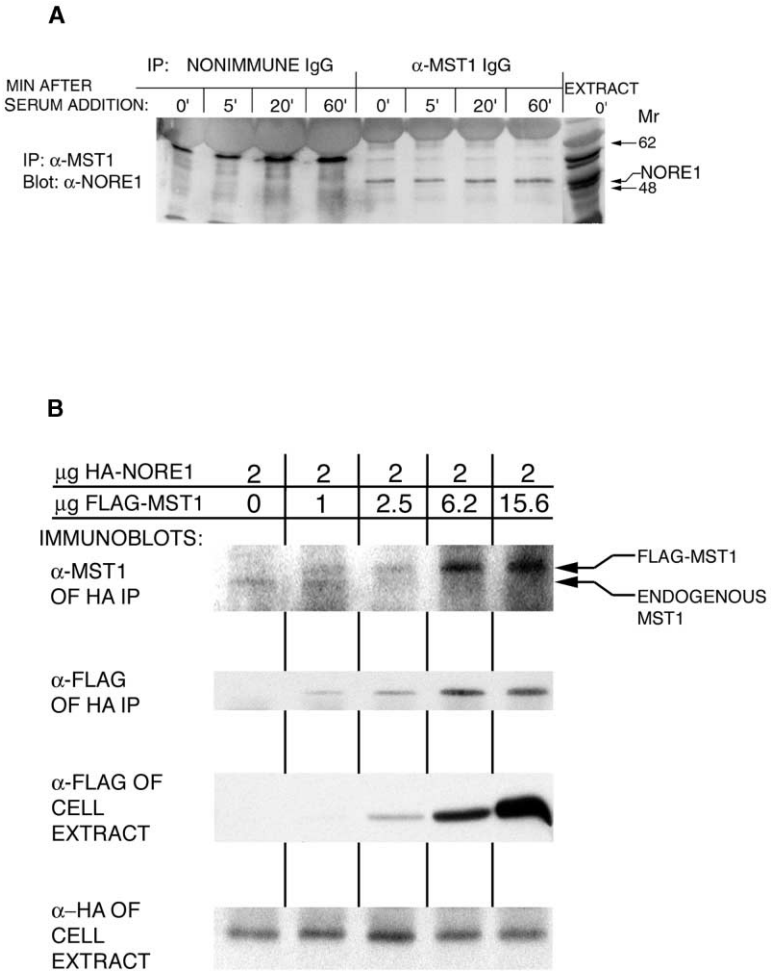

Figure 2. A NORE-MST1 Complex Exists In Vivo

(A) Endogenous NORE1 and MST1 form a constitutive complex in KB cells. KB cells were deprived of serum for 24 hr; fetal calf was added to 10%, and cells were sampled thereafter at the times indicated. Aliquots of the cell extracts were incubated with normal goat IgG or goat anti-MST1 IgG as indicated. After harvest on protein A/G beads, extensive washing, and SDS PAGE, the recovered proteins were subjected to immunobloting with a rabbit polyclonal anti-NORE1 antibody described in [13]. Right lane, KB cell extract.

(B) Endogenous MST1 binds recombinant HA-NORE1 and is displaced by excess recombinant MST1. COS-7 cells were transfected with vectors encoding a constant amount of HA-NORE1 and FLAG vector or increasing amounts of FLAG-MST1. The HA-NORE was recovered from cell extracts by immunoprecipitaion with anti-HA antibody 12CA5 and was subjected to immunobloting for MST1 and FLAG as indicated. Top panel: proteins recovered in the αHA immunoprecipitates probed with anti-MST1 antibody. Second panel: proteins recovered in the αHA immunoprecipitates probed with anti-FLAG antibody. Third panel: cell extracts probed with anti-FLAG antibody; note the increasing expression of FLAG-MST1. Lowest panel: cell extracts probed with anti-HA antibody.

polyclonal anti-NORE antibodies (Figure 2A), only the 46-kDa band was recovered in anti-cRas (Y13-238) immunoprecipitates, and only after serum stimulation [13]. As shown in Figure 2A, anti-MST1 immunoprecipitates prepared from KB cells also contain the 46-kDa NORE polypeptide whose presence is unaffected by serum deprivation/stimulation (Figure 2A).

Our polyclonal anti-NORE antibodies do not enable reliable immunoprecipitation of endogenous NORE. We therefore expressed recombinant HA-tagged NORE and probed the HA immunoprecipitate for endogenous MST1; in addition, FLAG-tagged MST1 was expressed simultaneously in increasing amounts. As seen in Figure 2B, an immunoreactive band is observed in the αMST1 immunoblot of the HA-NORE immunoprecipitate that is identical in mobility to the MST1 band observed in the cell extract. Moreover, the increasing expression of the slightly larger FLAG-MST1 is accompanied by the appearance of increasing amounts of a slightly larger αMST1-reactive polypeptide in the HA-NORE immunoprecipitates, which ultimately displaces entirely the endogenous MST1 polypeptide. Thus, MST1 and NORE form a complex in vivo, which is constitutive (or at least insensitive to serum withdrawal/addition) and saturable.

Active Ras Binds the NORE-MST1 Complex In Vivo

We next determined whether the NORE-MST1 complex is able to interact with active Ras. A constant amount of FLAG-tagged Ha-RasG12V was expressed with a constant level of FLAG-tagged NORE and increasing amounts of FLAG-tagged MST1. The FLAG-tagged Ha-RasG12V was precipitated with the anti-Ras antibody Y13-238, and the initial cell extracts and the Ras IPs were probed for FLAG-tagged polypeptides (Figure 3A). As seen in the upper panel, the FLAG-MST1 polypeptide is recovered in the RasG12V immunoprecipitate, but only in the presence of coexpressed NORE. Moreover, by comparing the intensities of FLAG-NORE and FLAG-MST1 in the cell extract to that of the Ras IP, it can be estimated that, in the presence of an excess of RasG12V, about 20% of both FLAG-NORE and coexpressed FLAG-MST1 are recovered in the RasG12V immunoprecipitate. Thus active Ras is able to bind the NORE-MST1 complex. GST-NORE and GST Raf (1–257) each bind in vitro slightly better to Ki-RasG12V than to Ha-RasG12V, whereas GST RASSF1A binds neither Ras polypeptide (Figure 3B). We showed previously that the Ras binds NORE through the Ras effector loop; mutation of Ras Asp38 to Ala or Asn abolishes Ras binding to NORE [13]. Here, we examine the ability of several other Ha-RasG12V effector loop mutants to bind NORE during transient expression (Figure 3C). The mutation Ha-RasT35S greatly diminishes, and Y40C abolishes, the HA-RasG12V-NORE interaction; conversely, the Ha-RasG12V, E37G mutant exhibits unimpaired (and perhaps enhanced) binding to NORE.

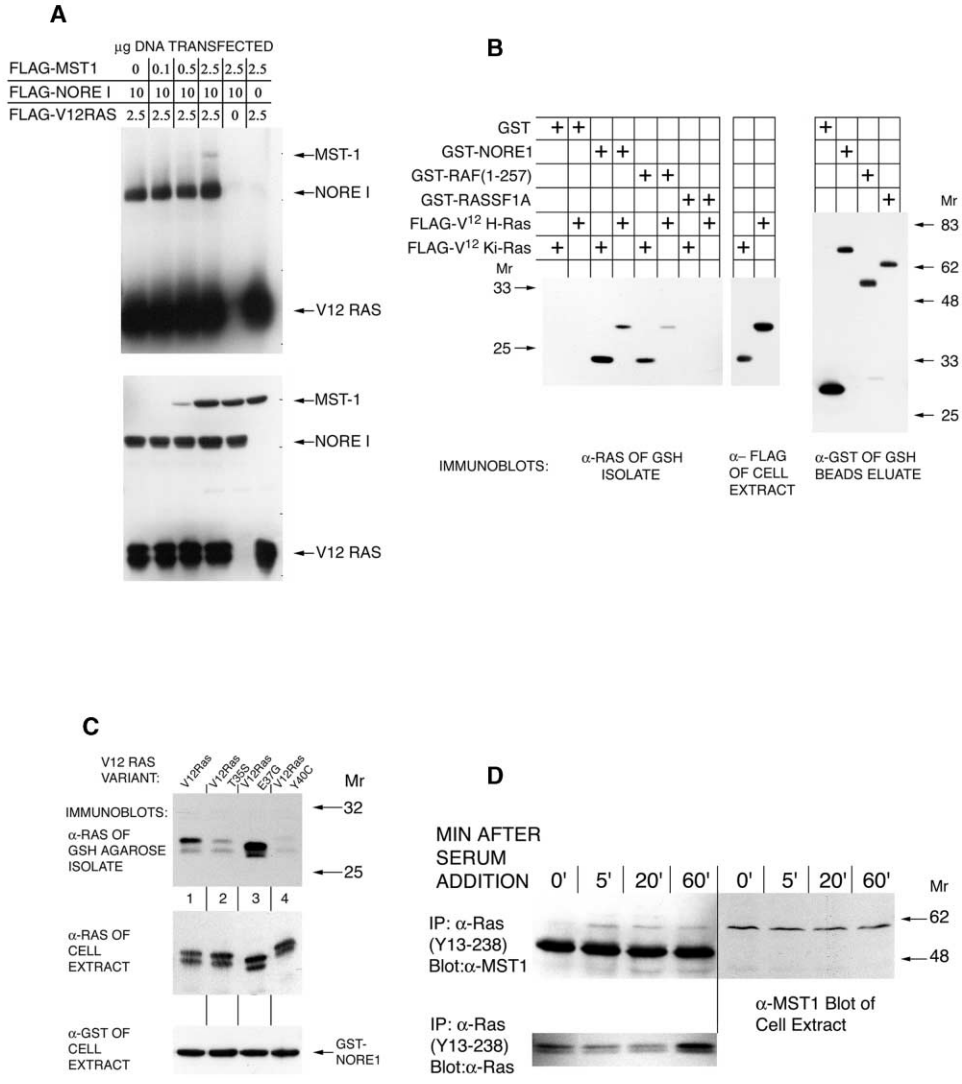

Figure 3. Active Ras Recruits the NORE-MST1 Complex

(A) RasG12V binds MST1 through NORE1. COS-7 cells were transfected with vectors encoding FLAG-tagged versions of MST1, NORE1, and HA-RasG12V, using the amounts indicated; each transfection contained 15 μg DNA. Aliquots of the cell extracts were mixed with anti-Ras Y13-238 monoclonal antibody coupled to agarose beads (Santa Cruz). After extensive washing and SDS PAGE, the polypeptides recovered by Y13-238 (upper panel) and aliquots of the cell extract (lower panel) were subjected to anti-FLAG immunobloting.

(B) Relative binding of HA-RasG12V and Ki-RasG12V to NORE1, RASSF1A, and Raf (1–257) in vitro. HEK293 cells were transfected with pEBG (encoding GST) or pEBG-NORE (7–413) or pEBG Raf (1–257) or pEBG RASSF1A. Aliquots from extracts of these cells containing comparable amounts of GST and each of the GST fusion proteins were adsorbed to GSH-agarose. pCMV5 encoding either FLAG Ki-RasG12V or FLAG Ha-RasG12V were expressed separately in HEK293 cells. Aliquots of extracts from these cells (as shown in the center panel) were adsorbed to the immobilized GST proteins; the beads were washed extensively and eluted with SDS. The left panel shows an anti-Flag immunoblot, and the right panel shows an anti-GST blot of this SDS eluate.

(C) Binding of NORE1 to HA-RasG12V with a normal or mutant effector loop. HEK293 cells were transfected with HA-tagged Ha-Ras mutants G12V (lane 1), G12V T35S (lane 2), G12V E37G (lane 3), or G12V Y40C (lane 4) together with GST-NORE1 (7–413). The latter was isolated from cell extracts on GSH-agarose, washed, and analyzed by immunoblotting after SDS PAGE. Upper panel: proteins retained on GSH beads were probed with mouse anti-Ras antibody (AB-2, Calbiochem). Middle panel: cell extracts probed with anti-Ras antibody. Lower panel: cell extracts probed with anti-GST antibody.

(D) Serum induces the association of endogenous MST1 with endogenous cRas. KB cells were deprived of serum for 24 hr and then stimulated by the addition of fetal calf serum to 10%; cells were sampled before and at the indicated times after serum readdition. Aliquots of the cell extracts were mixed with anti-Ras Y13-238 antibody coupled to agarose beads (Santa Cruz). The cell extracts and the washed beads were subjected to SDS PAGE and analyzed by immunoblotting, as indicated. Upper panel, left four lanes: proteins recovered with αRas Y13-238 immunoblotted with anti-MST1 antibody (Zymed); upper panel, right four lanes: cell extract immunoblotted with anti-MST1 antibody. Lower panel: Y13-238 immunoprecipitates immunoblotted with mouse anti-Ras antibody (AB-2, Calbiochem).

The ability of endogenous Ras to bind endogenous MST1 was evaluated in KB cells. Endogenous cRas was immunoprecipitated from cell extracts prepared from serum-deprived KB cells and at several times after serum addition; the anti-Ras (Y13-238) IPs were probed for MST1. A band of immunoreactive MST1 is observed in the cRas IPs only after serum addition and persists for up to 1 hr (Figure 3D); this is similar to the serum-induced association of endogenous NORE with cRas reported previously [13]. Thus, serum-induced activation of endogenous Ras causes the recruitment of the NORE-MST1 complex to the Ras effector loop.

Membrane Recruitment of MST1 Promotes Its Apoptotic Action

We sought next to define the functional significance of the Ras-NORE-MST1 interaction to the pleiotypic array of cellular responses mediated by Ras. The immediate downstream targets of MST1 are unknown; however, it has been consistently observed that overexpression of recombinant MST1 results in apoptosis in a number of cell backgrounds [37–39]. Although the pathway by which MST1 promotes apoptosis is unknown, we chose to employ apoptosis as a quantifiable measure of the efficacy of MST1 action in vivo.

As expected from previous reports, transient expression of MST1 results in apoptosis in several cell types, measured either as an increase in Annexin V surface binding (Figure 4A) or as a decrease in the percent survival of transfected cells (Figures 4B and 4C). An initial series of studies was carried out in NIH3T3 cells (Figure 4A); overexpression of MST1 gave a 2-fold increase in the fraction of cells staining with Annexin V at 24 hr after transfection, whereas MST1 (KR) gave no alteration as compared to vector control. NORE alone caused a statistically significant but very small increase in Annexin V staining of NIH3T3 cells, and the combined expression of NORE and MST1 yielded Annexin V staining slightly (but not significantly) less than that seen with MST1 alone. By contrast, NORECAAX causes a doubling in the fraction of Annexin V-positive cells, and coexpression of MST1 with NORECAAX resulted in an increase in the fraction of Annexin V-stained cells that was significantly (about 50%) greater than the sum of the effects of MST1 and NORECAAX individually (Figure 4A) and (in two experiments) comparable to the proapoptotic effect of Baxα (data not shown). The ability of NORECAAX and MST1 to promote Annexin V staining was fully suppressed by inclusion of zVAD-FMK in the medium after transfection (Figure 4D). A similar pattern of responses to NORE and NORECAAX, singly and in combination with MST1, was seen in Jurkat (Figure 4B) and HEK293 cells (Figure 4C). In both cells' backgrounds, MST1 (but not the inactive MST1 KR mutant) and NORECAAX caused a dose-dependent (examined in Jurkat only) increase in apoptosis, and the combination of low doses of NORECAAX with MST1 caused additive (Jurkat) or superadditive (HEK293) killing, which was suppressed by the presence of BV p35 CrmA plus BclX_L or incubation with zVAD-FMK (data not shown).

The ability of NORECAAX to augment the response to MST1 suggested that the recruitment of MST1 to the membrane enhanced its apoptotic action. To examine this idea, the amino-terminal myristoylation and polybasic segment of cSrc [40] was fused onto the N terminus of MST1. Although myristoylation (or coexpression with excess NORECAAX) tends to decrease MST1 polypeptide expression per μg of MST1 cDNA in comparison to MST1 alone, the apoptotic efficacy (per μg DNA) of myrMST1 was about 2-fold greater than MST1 in NIH3T3 cells. In addition, side-by-side comparisons in NIH3T3 cells suggest that apoptosis induced by myrMST1 is about 50% less than by MST1 coexpressed with NORECAAX (Figure 4A). In Jurkat cells, the efficacy of myrMST1 was only slightly greater than MST1 itself and much less than that of MST1 coexpressed with NORECAAX (Figure 4B); in contrast, the proapoptotic efficacy of myrMST1 in HEK293 cells (Figure 4C) was markedly greater than MST1, and in three experiments, only slightly less than MST1 coexpressed with NORECAAX.

Thus, the apoptotic effect of MST1 is generally increased by membrane targeting, either by myristoylation, or most consistently by coexpression with a membrane-targeted variant of NORE.

RasG12V Promotes Apoptosis through a NORE-MST1 Complex

The ability of Ras to recruit a NORE-MST1 complex, coupled with the increased apoptotic efficacy of membrane-targeted MST1, is consistent with the possibility that the NORE-MST1 complex could act as a proapoptotic effector of constitutively active forms of Ras. We tested this idea using HEK293 cells, in view of the high-grade apoptosis observed with myrMST1 or NORECAAX plus MST1 in this cell background. Overexpression of Ki-RasG12V in 293 cells efficiently induces cell death (Figure 5A). In contrast, Ha-RasG12V gives no significant cell death, in spite of the consistently higher Ha-Ras polypeptide expression achieved when comparable levels of Ha-Ras and Ki-Ras DNA are transfected. The expression of Ki-RasG12V per se is sufficient to cause cell death, which becomes maximal at 48–72 hr; however, the time course of Ki-RasG12V-induced cell death is considerably accelerated by the addition after transfection of low amounts of proapoptotic agents like tamoxifen or staurosporine at concentrations below those capable of directly inducing apoptosis in HEK293 cells transfected with empty control vectors.

Although commonly considered interchangeable, a number of differences in the biologic responses to Ha-RasG12V and Ki-RasG12V have been observed previously [41]. Of particular note [42], Ha-RasG12V is considerably (7-fold) more effective in activating PI 3-kinase than is Ki-RasG12V. Reasoning that the greater ability of Ha-RasG12V to activate this major antiapoptotic effector may suppress the expression of a concomitant proapoptotic outflow, we examined the proapoptotic effect of the Ha-Ras effector loop mutant G12V, E37G, which is unable to bind PI 3-kinase and Raf yet remains competent to bind NORE (Figure 3C); Ha-RasG12V, E37G elicits substantial cell death in 293 cells, exhibiting perhaps 2/3 the potency of Ki-RasG12V (Figure 5A). The cell death elicited by Ki-RasG12V and Ha-RasG12V, E37G is inhibited by coexpression with the baculoviral

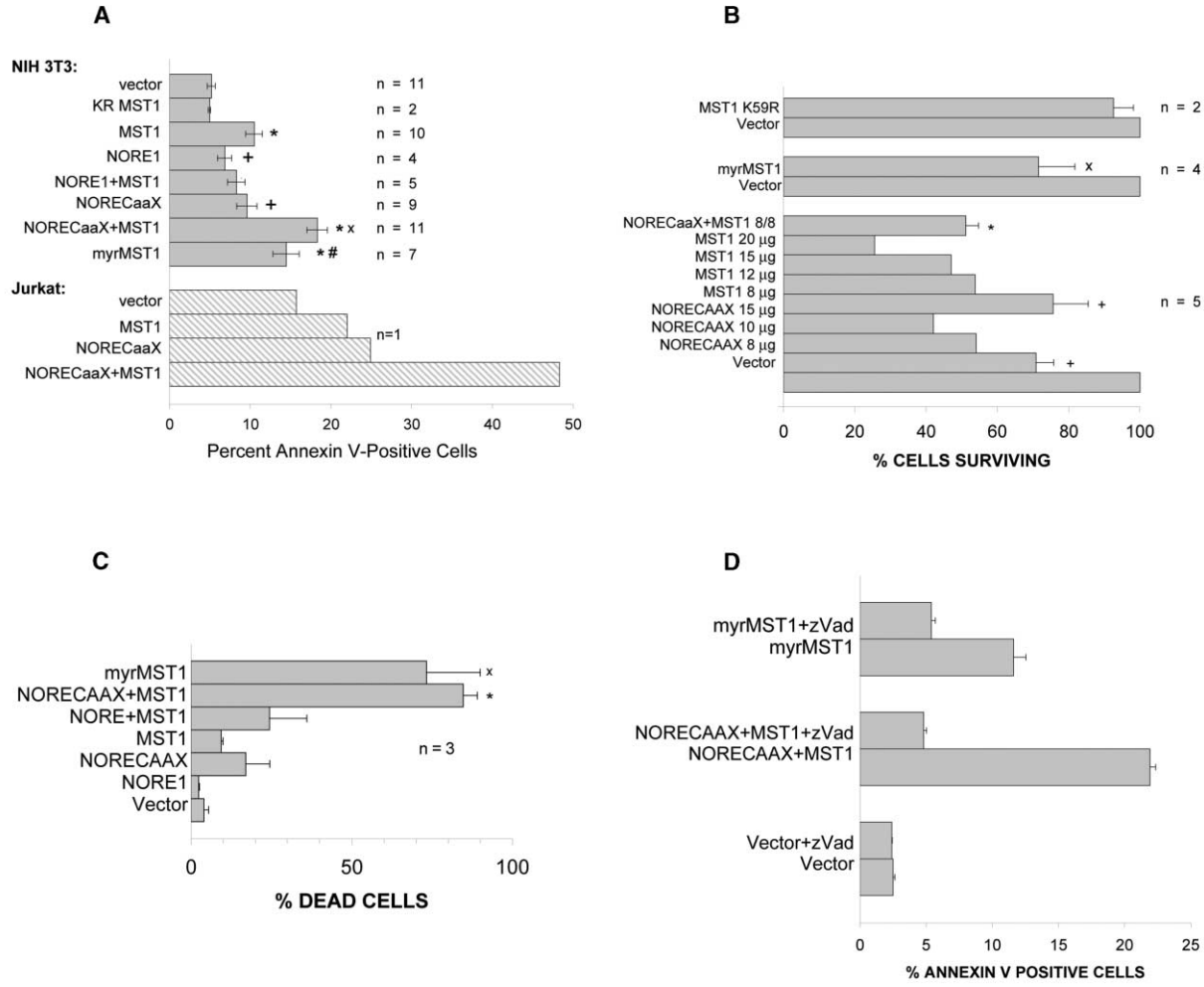

Figure 4. Membrane Recruitment Amplifies the Proapoptotic Effect of MST1

(A) The effects of NORE and MST1 on Annexin V surface binding in NIH3T3 and Jurkat cells. The number of observations for each condition is indicated. Where $n \geq 3$, the SE is shown; where $n = 2$, the error bars indicate the range of values. An asterisk indicates that $p < .001$ versus vector; a plus sign indicates that $p < .01$ versus vector; a multiplication sign indicates that $p < .001$ versus MST; a number sign indicates that $p < .05$ versus MST. The efficiency of NIH3T3 transfection was about 33%, as determined by counting GFP-positive cells transfected with a GFP reporter. The Jurkat data are from a single experiment; additional Jurkat experiments, analyzed by second method, are shown in Figure 4B.

(B) The effects of NORE and MST1 on the survival of Jurkat Tag cells. Three series of experiments are shown; the number (n) of individual experiments is indicated. In the series shown as $n = 5$, this number of observations applies only to the transfection of 8 μg cDNA for MST1 and NORECAAX; the cell survival values indicated for MST1, 12–20 μg, and NORECAAX, 10 and 15 μg, represent the average of two experiments, and no error bars are shown for these values. The comparison of MST1 (K59R) to vector was done twice; the error bar represents the range of values observed. Otherwise, SE are shown. An asterisk indicates that $p < 0.001$ versus vector; a plus sign indicates that $p < 0.01$ versus vector; a multiplication sign indicates that $p < 0.05$ versus vector.

(C) The effects of NORE and MST1 on cell death in HEK293 cells. A set of three experiments is summarized. The SE is shown. An asterisk indicates that $p < 0.001$ versus vector; a multiplication sign indicates that $p < 0.05$ versus vector.

(D) The caspase inhibitor zVAD-FMK suppresses NORE1 and MST1-induced Annexin V binding. NIH3T3 cells were transfected in duplicate with vectors encoding either NORECAAX together with wild-type MST1, or with myrMST1. zVAD-FMK (42 μM) was added at the time of transfection, as indicated. The cells were harvested 24 hr later, stained with Annexin V-Alexa 488, and analyzed by FACS as described in the Experimental Procedures.

antiapoptotic protein p35 CrmA (Figure 5B and data not shown) or by preincubation with zVAD-FMK (data not shown). Moreover, although the appearance of HEK293 cells overexpressing Ha-RasG12V did not differ significantly from GFP controls, expression of Ki-RasG12V and Ha-RasG12V, E37G is accompanied by changes in cell morphology characteristic of apoptotic cell death, i.e., prominent membrane blebbing, loss of cytoarchitecture, and nuclear and cytoplasmic fragmentation resulting in apoptotic bodies (Figure 5C). In addition, coexpression of Ki-RasG12V with dominant inhibitory mutants of caspase 3, 6, 7, and 9 each substantially suppressed the Ki-RasG12V-induced cell death, whereas dominant inhibitory caspase 8 had no effect (Figure 5B). Thus, the cell death elicited by Ki-RasG12V and Ha-RasG12V, E37G in HEK293 cells reflects a caspase-mediated pro-

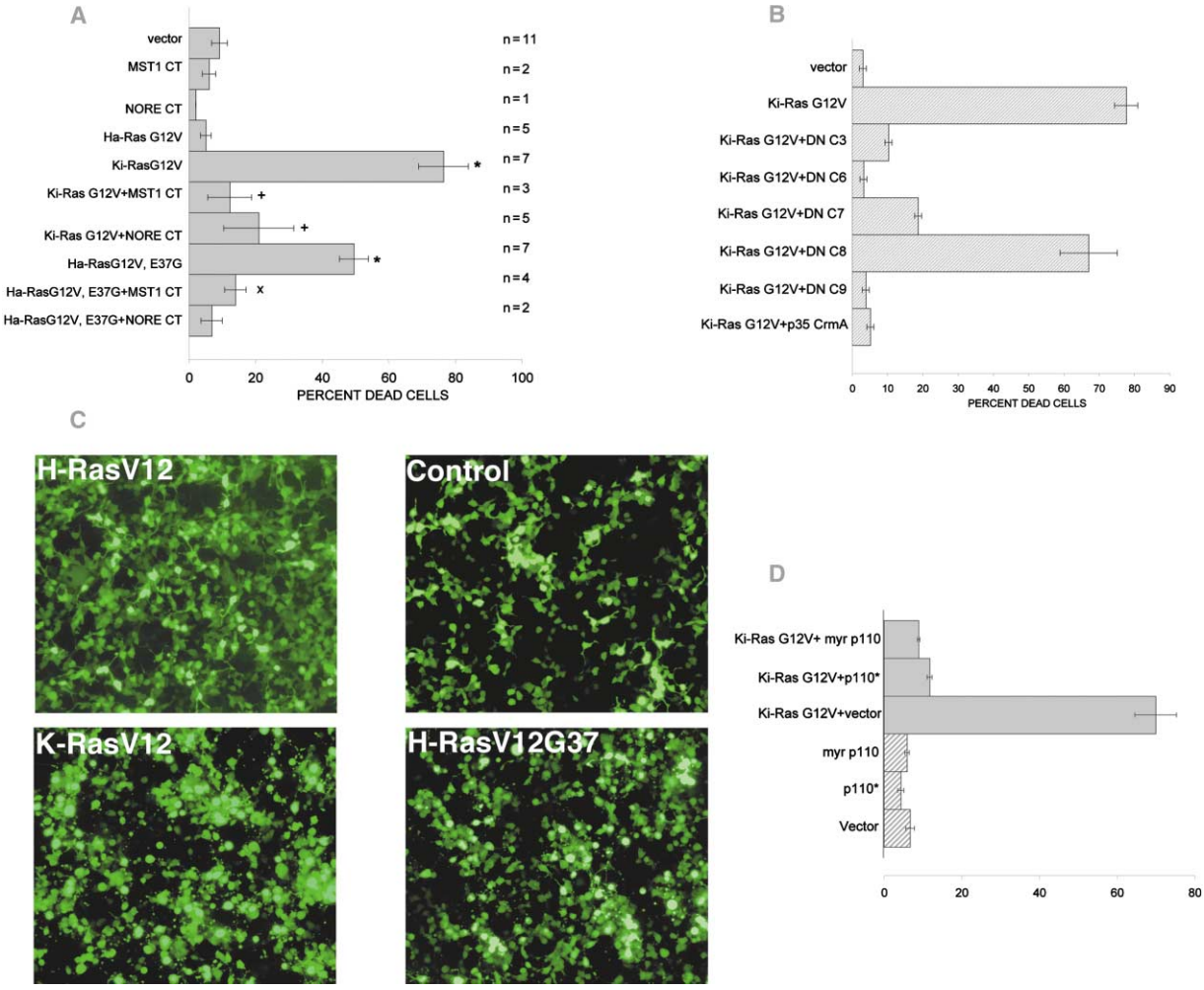

Figure 5. Ki-RasG12V and Ha-RasG12V, E37G Induce Apoptosis through a NORE-MST1 Complex

(A) Ki-RasG12V and Ha-RasG12V, E37G induce death in HEK293 cells, which is suppressed by interfering fragments of NORE and MST. The number of observations for each condition is indicated on the right. The SE is shown, except for n = 2, where error bars indicate the range of values. An asterisk indicates that $p < 0.001$ versus vector; a plus sign indicates that $p < 0.0001$ versus Ki-RasG12V; a multiplication sign indicates that $p < 0.001$ versus Ha-RasG12V, E37G.

(B) The effect of various caspase inhibitors on Ki-RasG12V induced death in HEK293 cells. Cells were transfected with empty vectors or vectors encoding Ki-RasG12V alone, or together with vectors encoding p35 CrmA catalytic inactive mutants of individual caspases: Caspase3 (DNC3), Caspase 6 (DNC6), Caspase7 (DNC7), Caspase 8 (DNC8), or Caspase 9 (DNC9). The error bars represent the SD of replicate determinations in a single experiment.

(C) The effect of RasG12V variants on the morphology of HEK293 cells. Subconfluent cultures were cotransfected with plasmids encoding enhanced GFP together with empty FLAG-pCMV5 or pCMV5 encoding Ha-RasG12V or Ki-RasG12V or Ha-RasG12V, E37G. The cells were maintained in the absence of tamoxifen or other proapoptotic agents and photographed 24 hr after transfection.

(D) Constitutively active variants of the PI 3-kinase catalytic subunit suppress Ki-RasG12V-induced apoptosis. The values shown are the mean and standard deviation of triplicate measurements from a single experiment. A second experiment gave similar results.

cess probably occurring primarily through activation of the "intrinsic" (i.e., TNF receptor superfamily- and caspase 8-independent) pathway. The apoptosis induced by Ki-RasG12V is potently suppressed by coexpression with constitutively active variants of the PI 3-kinase p110 catalytic subunit (Figure 5D).

We sought next to determine whether the ability of Ki-RasG12V and RasG12V, E37G to bind the NORE-MST1 complex was critical to their proapoptotic action. This was evaluated by examining whether overexpression of the segment of NORE responsible for binding MST1 (introduced as GST-NORE [358–413]) or the carboxy-terminal noncatalytic segment of MST1 (introduced as FLAG-MST1 [307–487]) were each able to interfere specifically with apoptosis induced by Ki-RasG12V and Ha-RasG12V, E37G (Figure 5A). Neither GST-NORE (358–413) nor FLAG-MST1 (307–487) expressed alone altered cell survival; conversely, expression of either fragment inhibited nearly completely the ability of Ki-RasG12V and Ha-RasG12V, E37G to induce apoptosis. The inhibitory action of the NORE and MST1 carboxy termini was specific for apoptosis initiated by RasG12V; neither the GST-NORE fusion nor the MST1 carboxy-terminal segment inhibited Fas-induced apo-

ptosis in the Jurkat cell background (data not shown). Thus, sequestration of MST1 (by GST-NORE [358–413]) or expression of the MST1 noncatalytic segment, which contains autoinhibitory, dimerization, and NORE binding domains, each inhibits selectively the ability of Ki-RasG12V and Ha-RasG12V, E37G to promote apoptosis.

MST1 Kinase Activity

We next inquired whether NORE and/or RasG12V regulate MST1 kinase activity. The readditon of serum to 293 or KB cells deprived overnight did not alter the activity of immunoprecipitated endogenous MST1. Cotransfection of MST1 (and in one experiment, MST2) with an excess of NORE was accompanied by an increase in MST1 expression; however, the specific activity of MST1 assayed in vitro was suppressed by up to 80% (see the Supplementary Material available with this article online). Serum readdition in the presence of coexpressed NORE did not cause significant alteration in the activity of recombinant MST1 or in its mobility on SDS PAGE. The coexpression of Ha- or Ki-RasG12V with MST1, or with a NORE-MST1 complex, gave no consistent change of MST1 activity (see the Supplementary Material). The apparent suppression of recombinant MST1 activity by coexpression with NORE and the absence of RasG12V-induced alteration in the activity of recombinant MST1, as well as the observation that serum induces the binding of an endogenous NORE-MST1 complex to endogenous Ras without detectably altering the catalytic activity of MST1 assayed in vitro, taken together suggest that Ras controls MST1 signaling primarily by its recruitment of MST1 to a site critical for MST1 action.

Discussion

NORE is a noncatalytic protein that binds Ras and several other GTPases in the Ras subfamily in a GTP-dependent manner in vitro and in vivo [13, 33]. The ability of serum and EGF to stimulate the association of NORE with both endogenous and recombinant Ras in several cell backgrounds supports the view that NORE is among Ras' physiologic effectors. Seeking evidence of NORE function, we were intrigued by the considerable (50%) identity in amino acid sequence between the carboxy-terminal 300 amino acids of NORE and the putative tumor suppressor protein RASSF1A, one of the longer (340 aa) splice variants of the RASSF1 gene. Moreover, the 300 amino acid homologous segments of NORE and RASSF1A are each 40% identical in amino acid sequence to a segment of the protein product of the *C. elegans* gene T24F1.3 (Figure 1A). We reasoned that this strong conservation in primary sequence indicated that one or more functions mediated by this segment were also strongly conserved. In as much as all three segments contain a Ras/Rap association (RA) domain, we considered it probable that this conserved function was binding to an active Ras-like GTPase. We were surprised however to discover that neither RASSF1 nor T24F1.3 exhibited any significant association with Ras or several Ras-like GTPases ([33] and Figure 3B). We next surveyed an array of NORE/RASSF1 interactors isolated by two-hybrid screens for their ability to bind all three NORE-related proteins and found that only the protein kinase MST1 exhibits such binding. Reciprocally, an extensive two-hybrid screen of a human lung cDNA library using MST1 as bait resulted in the recovery of all five of the known members of the NORE/RASSF gene family (i.e., NORE1, RASSF1,2,3, and Ado37), which, in aggregate, accounted for 30% of all MST1-interacting proteins recovered (Nedwidek et al., unpublished data). Thus, MST1 is a phylogenetically conserved partner of all NORE-related peptides. The function of T24F1.3 is unknown, and although RASSF1A is a candidate tumor suppressor [28, 29], its biochemical functions and the regulatory elements upstream of RASSF1A are also unknown. The ability of MST1 to engage in a ternary complex with Ras-GTP and NORE was consistent with the possibility that MST1 could act as a physiologic effector of Ras. We therefore chose to evaluate first the role of NORE-MST1 in Ras action.

Little is known concerning the substrates or immediate downstream targets of MST1/2; however, several reports have shown that overexpression of MST1 will promote apoptosis in a variety of cells [37–39]. We therefore utilized apoptosis as an indicator of the action of recombinant MST1 in vivo. In the three cell backgrounds examined in this study (NIH3T3, Jurkat, and HEK293) using different assays (Annexin V externalization; zVAD-FMK/BV p35-suppressible increase in cell permeability or nuclear fragmentation), we confirmed that MST1 causes a dose-dependent increase in apoptosis and found that fusion of the membrane-targeting amino-terminal myristoylation motif from cSrc onto MST1 increased its apoptotic efficacy, substantially in NIH3T3 and HEK293 cells and slightly in Jurkat cells. Moreover, fusion of the carboxy-terminal membrane-targeting motif from Ki-Ras4B onto the NORE carboxy terminus, to give NORECAAX, conferred on NORE the ability to induce apoptosis consistently in all three cell backgrounds. Moreover, coexpression of NORECAAX with MST1 (in NIH3T3 and HEK293 cells) yielded cell death in excess of the sum of both agents individually and equal or greater than that seen with myrMST1.

Seeking a model to test the role of endogenous NORE-MST1 in the proapoptotic actions of Ras, we examined the ability of transiently overexpressed RasG12V to promote apoptosis. We found that transiently overexpressed Ha-RasG12V gave little or no apoptosis in several cell backgrounds. Review of the literature indicated that Ha-RasG12V-induced apoptosis has been consistently observed only under circumstances of massive overexpression, e.g., Ha-RasG12V driven by an IPTG-inducible promoter in Rat1 or NIH3T3 cells [43] or by direct microinjection of plasmid-encoding Ha-RasG12V [26]. In contrast, overexpression of Ki-RasG12V in HEK293 cells gave robust apoptosis; substantial apoptosis was also induced by Ki-RasG12V in Jurkat cells (data not shown). Whereas differential effects of Ki-RasG12V and Ha-RasG12V on apoptosis have not been noted previously, differential effects of these two Ras homologs on other downstream responses are known [41, 43, 44]. The much weaker proapoptotic effect of Ha-RasG12V as compared with Ki-RasG12V could be due to weaker activation of a proapoptotic effector or to a stronger activation of an antiapoptotic outflow (or

both). The finding that Ha-RasG12V, E37G, an effector loop mutant that is unable to bind Raf or PI 3-kinase, elicits substantially greater apoptosis than Ha-RasG12V strongly supports the latter formulation. It is important to emphasize that, although the proapoptotic effect of Ki-RasG12V (and Ha-RasG12V, E37G; data not shown) is suppressed by coexpression with an active PI 3-kinase, Ras-induced apoptosis is not caused by poor or absent activation of an antiapoptotic output alone; rather, the proapoptotic effects of Ki-RasG12V and Ha-RasG12V, E37G are due to their ability to activate a proapoptotic stimulus that is not effectively counteracted by a concomitant antiapoptotic outflow. The interference experiments indicate strongly that the proapoptotic stimulus supplied by both Ki-RasG12V and Ha-RasG12V, E37G requires the participation of NORE and MST1. Thus, overexpression of the C-terminal segment of NORE that binds MST1 in vivo is sufficient to suppress almost completely the proapoptotic action of Ki-RasG12V and Ha-RasG12V, E37G. Similarly, overexpression of the C-terminal noncatalytic segment of MST1, which contains the MST1 autoinhibitory, dimerization, and NORE binding domains, also strongly suppresses the proapoptotic action of Ki-RasG12V and Ha-RasG12V, E37G. Thus, considerable evidence supports the conclusion that the ability of Ki-RasG12V and Ha-RasG12V, E37G to induce apoptosis is mediated by the endogenous NORE-MST1 complex.

Although the present data establish that Ki-RasG12V (and Ha-RasG12V, E37G) induces apoptosis in HEK293 cells through recruitment of the endogenous NORE-MST1 complex, we have no evidence as to the functions mediated by the "physiologic" recruitment of NORE-MST1 engendered by receptor activation of cRas (e.g., as in Figure 3D). A few reports have described a requirement for Ras activation in specific apoptotic scenarios, e.g., as in the TCR-induced expression of FasL [45] or in TNFα-induced apoptosis of murine L929 cells [46]. Alternatively, apoptosis induced by trophic factor withdrawal in some settings is accompanied by Ras activation and is inhibited by overexpression of Ras S17N [47, 48]. Whether cRas-GTP recruitment of NORE-MST1 participates in such proapoptotic phenomena is yet to be determined. Alternatively, the "physiologic" recruitment of NORE-MST1 by cRas-GTP may initiate downstream responses entirely unrelated to the initiation of apoptosis, and perhaps only the continuous and/or inappropriately intense signaling engendered by Ki-RasG12V in specific cell backgrounds results in apoptosis (Figure 6).

In contrast to the lack of information as to the physiologic role(s) of NORE-MST1, several observations suggest that the RASSF1-MST1 complex may function physiologically as a proapoptotic effector. The RASSF1A isoform is a candidate tumor suppressor, whose loss of function (e.g., in lung cancers) promotes malignant transformation [29]; a biochemical function as a proapoptotic effector is consistent with such a biologic role. Vos et al. [49] have recently reported that RASSF1 overexpression can itself promote apoptosis. Both RASSF1A and the shorter RASSF1C splice variant, which apparently lacks tumor-suppressing activity, bind MST1. Nevertheless, although neither RASSF1A or -C exhibit significant direct binding to Ras-GTP (Figure 3B) or to other Ras-like GTPases, we find that the RASSF1A isoform is able to heterodimerize with NORE and thereby bind to Ras-GTP indirectly [33]. Thus, recruitment of a RASSF1A-MST1 complex by an as yet unknown upstream regulator (?Ras) may enable the initiation of MST's apoptotic program (Figure 6).

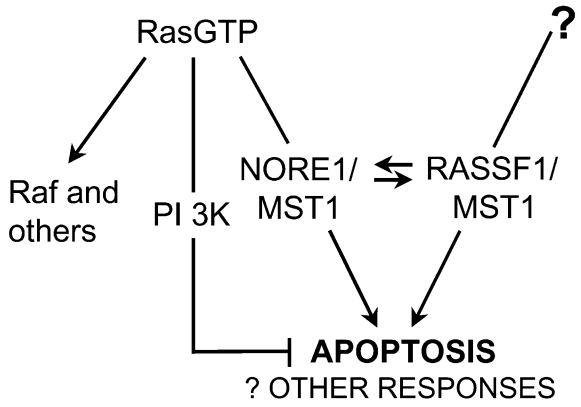

Figure 6. A Hypothesis for the Role of MST1 as an Effector of NORE and RASSF1

Whatever the role of NORE-MST1 in response to physiologic activation of Ras, the recruitment of NORE-MST1 by mutant active Ras is likely to be an important protective mechanism against Ras-induced transformation. The identification of a proapoptotic outflow from Ki-RasG12V raises the question of whether this property of constitutively active Ki-Ras can be exploited to enable the selective apoptosis of cells that have continuous high-grade Ras activation.

Experimental Procedures

DNA Constructs and Manipulations

Mouse MST1 cDNA was kindly provided by Dr. Leonard Zon (Children's Hospital, Boston, MA). cDNAs for human GCK and SOK protein kinases were kindly provided by Dr. John Kyriakis (Massachusetts General Hospital, Boston). cDNAs for human V12 Ha-Ras effector loop mutants E37G, T25S, and Y40C were kindly provided by Dr. Michael White (Southwestern Medical Center, Dallas, TX). RASSF1A and RASSF1C cDNAs were kindly provided by Dr. Gerd Pfeifer (Beckman Research Institute, City of Hope, CA). cDNAs encoding catalytically inactive caspase 3, 6, 7, 8, and 9 were provided by Dr. Dale Bredesen and constructed as described by Lu et al. [50]. The baculoviral p35 caspase inhibitor CrmA, encoded in pCS2+, was provided by Dr. Vincent Cryns. *C. elegans* cDNA encoding amino acids 247–601 of the T24F1.3 gene product was kindly provided by Dr. Y. Kohara (Japan). The Myc-tagged, constitutively active PI 3-kinase p110* was described previously [51]. Human MST2 cDNA was obtained by PCR on a placental library cDNA, with the primers corresponding to the 5′ and 3′ ends of the full-length cDNA.

cDNAs manipulations were performed using the standard molecular biology techniques [51]. Full-length and truncated NORE1, RASSF1A, RASSF1C, T24F1.3, MST1, and MST2 cDNAs, as well as Ki-RasG12V, Ha-RasG12V, and its effector loop mutants were subcloned into pCMV5 FLAG vector in-frame downstream of the FLAG epitope (*MDYKDDDDKNSA*). For some constructs, the FLAG epitope in pCMV5 was replaced with the influenza virus hemagglutinin epitope (HA, *MYPYDVPDYA*) by excising the FLAG epitope and promoter region from pCMV FLAG plasmid with SacI and EcoRI enzymes and replacing it with the synthetic oligonucleotide coding

for the promoter region followed by the HA epitope in-frame with the downstream sequences. The same approach was used for the creation of the myristoylated MST1 and NORE1; the FLAG tag of the pCMV 5 was replaced with the cSrc myristoylation and polybasic segment (*MGSSKSKPKDPSQRRR*), followed by four glycine residues and an in-frame FLAG tag. The same approach was used to construct the myristoylated PI 3-kinase catalytic subunit (myr-p110). The p110* was digested with BamH1, releasing a 2.8-kb insert encoding full-length p110 with a C-terminal Myc epitope. This was inserted in-frame downstream of the cSrc myristoylation and polybasic segment and FLAG epitope in the pCMV5 vector. The fusion of the carboxy-terminal Ki-Ras4B membrane-association segment (CAAX, *SKDGKKKKKKSKTKCVIMstop*) onto the NORE carboxy terminus to create NORECAAX was accomplished by PCR, using a wild-type NORE template, replacing the NORE stop codon with the first amino acid(s) of the CAAX segment. The C-terminal pieces of NORE1 (358–413) and MST1 (456–488) were subcloned in- frame downstream of the GST moiety in the pEBG vector [13] by using the synthetic oligonucleotide (MST1) or PCR (NORE1) approaches. RASSF1A and Ha-RasG12V were cloned into pEBG by shuffling coding sequences from corresponding FLAG-tagged vectors. All other constructs were described in [13]. All point mutants were made using the QuickChange kit (Stratagene). All constructs were verified by DNA sequence analysis.

Apoptosis Assays

Annexin V Labeling in NIH3T3 Cells

The assay was performed as described in [52], with some modifications. NIH3T3 cells were plated at 3–4 $\times$ 10^5 per well in a 6-well plate the day before transfection. Cells were transfected in duplicate with 6 μg DNA and 10 μl Lipofectamine 2000 (GIBCO) in the presence of 10% serum, as recommended by the manufacturer, and left for 19–23 hr. In some experiments, zVAD-FMK (Calbiochem) was added to 42 μM (final concentration) at the time of transfection. Rat Annexin V, purified from liver or recombinant, labeled with Alexa 488 dye was added to the culture media to 1 mg/ml, and cells were incubated for 5 min at 37°C, followed by 25 min at room temperature in the dark. Media with floating cells was transferred to 5-ml centrifuge tubes on ice; the plates were washed twice with 1 ml HBS (20 mM HEPES [pH 7.4], 150 mM NaCl, 2.5 mM $CaCl_2$), and the washes were added to the tubes with media. Floating cells were pelleted, resuspended in 3 ml HBS, and pelleted again. Adherent cells were scraped into 1 ml HBS, pooled with floating cells from the same dish, and resuspended by vortexing. As Jurkat cells were maintained in suspension, the Annexin V labeling and washing was carried out as with the "floating" NIH3T3 cells. Cells were analyzed by Coulter EPICS V XL flow cytometer; the percent of Annexin V-positive cells was calculated by the cytometer software. Rat Annexin V was purified from frozen rat livers (Pel-Freeze, AR) as described [53] and labeled with Alexa 488 using the Molecular Probes Alexa fluor 488 protein-labeling kit according to manufacturer's instructions. In some experiments, the recombinant Annexin V used was a kind gift of Dr. M. Schlissel, UC, Berkeley, which we labeled with Alexa 488.

The Jurkat/T antigen cell line was cultured in complete IMDM medium supplemented with 10% FCS, 2 mM glutamine, and gentamycin (50 μg/ml) in a humidified incubator with 5% CO_2 in air at 37°C. The cells were kept at a density of 0.5–1 $\times$ 10^6/ml. Aliquots containing 3 $\times$ 10^6 Jurkat cells were electroporated at 250V and 960 μF with mixtures of plasmids, as indicated in the figures, together with 1 μg cDNA encoding GFP. At 24 hr posttransfection, cell survival was analyzed by flow cytometry using a previously optimized program to measure the percentage of live cells that are GFP positive present in forward scatter/side scatter gate in each experimental condition [54]. The vital GFP-positive cells were selected on the basis of unchanged scatter signals when compared to untransfected cells, and the apoptotic cell population with decreased FS and increased SS was excluded from the analysis. The data were expressed as "percent cells surviving", with vector controls set to 100%.

Apoptosis assays in HEK 293T cells were carried out as described previously [55, 56]. Cells were maintained in Dulbecco's modified Eagle's medium (DMEM) containing 10% fetal bovine serum (FBS). Transient transfections were performed using Lipofectamine (GIBCO-BRL) according to the manufacturer's instructions. A total of 2.5 $\times$ 10^5 293 T cells were seeded in each well of 24-well plates 1 day prior to transfection. Each well was transfected with a total of 0.5 μg DNA and 3.5 μl Lipofectamine. After 1 day of incubation, the proapoptotic agent tamoxifen was added at a final concentration of 20–25 μM to increase the rate of apoptosis. Floating cells were collected at 20–24 hr after the addition of tamoxifen, and cell death was assessed by trypan blue exclusion as before [55, 56].

Supplementary Material

Supplementary Material including data regarding the regulation of endogenous and recombinant MST kinase activity by serum withdrawal and readdition and by coexpression with NORE1 and active mutants of Ha- and Ki-Ras is available at http://images.cellpress.com/supmat/supmatin.htm.

Acknowledgments

We thank V. Cryns, J. Kyriakis, Y. Kohara, G. Pfeiffer, M. Schlissel, M.A.White, and L. Zon for providing DNA constructs, Yi Yin for technical assistance, Demetrios Vavvas for initial experiments suggesting NORE function in apoptosis, Sara Ortiz and Alexei Mikhailov for help with figures, and Jeanette Prendable for typing the manuscript. This study was supported in part by a grant from Eli Lilly to J.A. A.K. was supported by a postdoctoral fellowship from The Leukemia and Lymphoma Society. R.X. was supported by National Institutes of Health grant AI 01472 and by the Center for Inflammatory Bowel Disease. S.R. was supported in part by Fellowship DRG-1620 of the Cancer Research Fund of the Damon Runyon-Walter Winchell Foundation. X.-F.Z. was supported by National Institutes of Health grant GM51281.

Received: October 29, 2001
Revised: January 1, 2002
Accepted: January 2, 2002
Published: February 19, 2002

References

1. Shields, J.M., Pruitt, K., McFall, A., Shaub, A., and Der, C.J. (2000). Understanding Ras: "it ain't over 'til it's over". Trends Cell Biol. *4*, 147–154.
2. Marshall, M. (1993). The effector interactions of p21 ras. Trends Biochem. Sci. *18*, 250–254.
3. Avruch, J., Khokhlatchev, A., Kyriakis, J.M., Luo, Z., Tzivion, G., Vavvas, D., and Zhang, X.F. (2001). Ras activation of the Raf kinase: tyrosine kinase recruitment of the MAP kinase cascade. Recent Prog. Horm. Res. *56*, 127–155.
4. Bos, J. (1989). Ras oncogenes in human cancer: a review. Cancer Res. *49*, 4682–4689.
5. Oldham, S.M., Clark, G.J., Gangarosa, L.M., and Coffey, R.J., Jr. (1996). Activation of the Raf-1/MAP kinase cascade is not sufficient for Ras transformation of RIE-1 epithelial cells. Proc. Natl. Acad. Sci. USA *93*, 6924–6928.
6. White, M.A., Nicolette, C., Minden, A., Polverino, A., Van Aelst, L., Karin, M., and Wigler, M.H. (1995). Multiple Ras functions can contribute to mammalian cell transformation. Cell *80*, 533–541.
7. Joneson, T., White, M.A., Wigler, M.H., and Bar-Sagi, D. (1996). Stimulation of membrane ruffling and MAP kinase activation by distinct effectors of RAS. Science *271*, 810–812.
8. Taylor, S.J., and Shalloway, D. (1996). Cell cycle-dependent activation of Ras. Curr. Biol. *6*, 1621–1627.
9. Rodriquez-Viciana, P., Warne, P.H., Vanhaesebroeck, B., Waterfield, M.D., and Downward, J. (1996). Activation of phosphatide 3-kinase by interaction with Ras and by point mutation. EMBO J. *15*, 2442–2451.
10. Wolthus, R.M., and Bos, J.L. (1999). Ras caught in another affair; the exchange factors for Ral. Curr. Opin. Genet. Dev. *1*, 112–117.
11. Kuriyama, M., Harada, N., Kuroda, S., Yamamoto, T., Nakafuku, M., Iwamatsu, A., Yamamoto, D., Prasad, R., Croce, C., Canaani, E., et al. (1996). Identification of AF-6 and canoe as putative targets for Ras. J. Biol. Chem. *271*, 607–610.
12. Han, L.M., and Colicelli, J. (1995). A human protein selected for

interference with Ras functions interacts directly with Ras and competes with Raf. Mol. Cell. Biol. *15*, 1318–1323.
13. Vavvas, D., Li, X., Avruch, J., and Zhang, X.F. (1998). Identification of NORE1 as a potential Ras effector. J. Biol. Chem. *273*, 5439–5442.
14. Newbold, R.F., and Overell, R.W. (1983). Fibroblast immortality is a prerequisite for transformation by EJ C-Ha-ras oncogene. Nature *304*, 648–651.
15. Hirakawa, T., and Ruley, H.E. (1988). Rescue of cells from ras oncogene-induced growth arrest by a second, complementing, oncogene. Proc. Natl. Acad. Sci. USA *85*, 1519–1523.
16. Ridley, A.J., Paterson, H.F., Noble, M., and Land, H. (1988). Ras-mediated cell cycle arrest is altered by nuclear oncogenes to induce Schwann cell transformation. EMBO J. *7*, 1635–1645.
17. Lui, X., Park, S.H., Thompson, T.C., and Lane, D.P. (1992). Ras-induced hyperplasia occurs with mutation of p53, but activated ras and myc together can induce carcinoma without p53 mutation. Cell *70*, 153–161.
18. Lloyd AC. (1998). Ras versus cyclin-dependent kinase inhibitors. Curr. Opin. Genet. Dev. *8*, 43–48.
19. Serrano, M., Lin, A.W., McCurrach, M.E., Beach, D., and Lowe, S.W. (1997). Oncogenic ras provokes premature cell senescence associated with accumulation of p53 and p16 ^{INK4a}. Cell *88*, 593–602.
20. Downward, J. (1998). Ras signaling and apoptosis. Curr. Biol. *8*, 49–54.
21. Frame, S., and Balmain, A. (2000). Integration of positive and negative growth signals during ras pathway activation in vivo. Curr. Opin. Genet. Dev. *10*, 106–113.
22. Palmero, I., Pantoja, C., and Serrano, M. (1998). p19 ARF links the tumour suppressor p53 to Ras. Nature *395*, 125–126.
23. Bates, S., Phillips, A.C., Clark, P.A., Stott, F., Peters, G., Ludwig, R.L., and Vousden, K.H. (1998). P14^{ARF} links the tumour suppressors RB and p53. Nature *395*, 124–125.
24. Fukasawa, K., and Vande Woude, G.F. (1997). Synergy between the Mos/mitogen-activated protein kinase pathway and loss of p53 function in transformation and chromosome instability. Mol. Cell. Biol. *17*, 506–518.
25. Mayo, M.W., Wang, C.Y., Cogswell, P.L., Rogers-Graham, K.S., Lowe, S.W., Der, C.J., and Baldwin, A.S., Jr. (1997). Requirement of NFκ-B activation to suppress p53-independent apoptosis induced by oncogene Ras. Science *278*, 1812–1815.
26. Joneson, T., and Bar-Sagi, D. (1999). Suppression of Ras-induced apoptosis by the Rac GTPase. Mol. Cell. Biol. *19*, 5892–5901.
27. Liou, J.S., Chen, C.Y., Chen, J.S., and Faller, D.V. (2000). Oncogenic Ras mediates apoptosis in response to protein kinase C inhibition through the generation of reactive oxygen species. J. Biol. Chem. *275*, 39001–390011.
28. Lerman, M.I., and Minna, J.D. (2000). The 630-kb lung cancer homozygous deletion region on human chromosome 3p21.3: identification and evaluation of the resident candidate tumor suppressor genes. Cancer Res. *60*, 6116–6133.
29. Dammann, R., Li, C., Yoon, J.H., Chin, P.L., Bates, S., and Pfeifer, G.P. (2000). Epigenetic inactivation of a Ras association domain family protein from the lung tumour suppressor locus 3p21.3. Nat. Genet. *25*, 315–319.
30. Burbee, D.G., Forgacs, E., Zochbauer-Muller, S., Shivakumar, L., Fong, K., Gao, B., Randle, D., Kondo, M., Virmani, A., and Bader, S. (2001). Epigenetic inactivation of RASSF1A in lung and breast cancers and malignant phenotype suppression. J. Natl. Cancer Inst. *93*, 691–699.
31. Dammann, R., Yang, G., and Pfeifer, G.P. (2001). Hypermethylation of the CpG island of Ras association domain family 1A (RASSF1A), a putative tumor suppressor gene from the 3p21.3 locus, occurs in a large percentage of human breast cancers. Cancer Res. *61*, 3105–3109.
32. Dreijerink, K., Braga, E., Kuzmin, I., Geil, L., Duh, F.M., Angeloni, D., Zbar, B., Lerman, M.I., Stanbridge, E.J., and Minna, J.D. (2001). The candidate tumor suppressor gene, RASSF1A, from human chromosome 3p21.3 is involved in kidney tumorigenesis. Proc. Natl. Acad. Sci. USA *98*, 7504–7509.
33. Ortiz-Vega, S., Khoklatchev, A., Nedwidek, M., Zhang, X.-F., Damman, R., Pfeifer, G., and Avruch, J. (2001). The putative tumor supressor RASSF1A homodimerizes and heterodimerizes with the Ras-GTP binding protein, Nore1. Oncogene, in press.
34. Creasy, C.L., and Chernoff, J. (1995). Cloning and characterization of a human protein kinase with homology to Ste20. J. Biol. Chem. *270*, 21695–21700.
35. Taylor, L.K., Wang, W.-C.R., and Erikson, R.L. (1996). Newly identified stress-responsive protein kinases, Krs-1 and Krs-2. Proc. Natl. Acad. Sci. USA *93*, 10099–10104.
36. Dan, I., Watanabe, N.M., and Kusumi, A. (2001). The Ste20 group kinases as regulators of MAP kinase cascades. Trends Cell Biol. *11*, 220–230.
37. Graves J.D., Gotoh, Y., Draves, K.E., Ambrose, D., Han, D.K., Wright, M., Chernoff, J., Clark, E.A., and Krebs, E.G. (1998). Caspase-mediated activation and induction of apoptosis by the mammalian Ste20-like MST1. EMBO J. *17*, 2224–2234.
38. Lee, K.K., Murakawa, M., Nishida, E., Tsubuki, S., Kawashima, S., Sakamaki, K., and Yonehara, S. (1998). Proteolytic activation of MST1/Krs, STE20-related protein kinase by caspase during apoptosis. Oncogene *16*, 3029–3037.
39. Graves, J.D., Draves, K.E., Gotoh, Y., Krebs, E.G., and Clark, E.A. (2001). Both phosphorylation and Caspase-mediated cleavage contribute to regulation of the Ste20-like protein kinase Mst1 during CD95/Fas-induced apoptosis. J. Biol. Chem. *276*, 14909–14915.
40. Reuther, G.W., Buss, J.E., Quilliam, L.A., Clark, G.J., and Der, C.J. (2000). Analysis of function and regulation of proteins that mediate signal transduction by use of lipid-modified plasma membrane-targeting sequences. Methods Enzymol. *327*, 331–350.
41. Ellis, C.A., and Clark, G. (2000). The importance of being K-Ras. Cell. Signal. *12*, 425–434.
42. Yan, J., Roy, S., Apolloni, A., Lane, A., and Hancock, J.F. (1998). Ras isoforms vary in their ability to activate Raf-1 and phosphoinositide 3-kinase. J. Biol. Chem. *273*, 24052–24056.
43. Shao, J., Sheng, H., DuBois, R.N., and Beauchamp, R.D. (2000). Oncogenic Ras-mediated cell growth arrest and apoptosis are associated with increased ubiquitin-dependent cyclin D1 degradation. J. Biol. Chem. *275*, 22916–22924.
44. Voice, J.K., Klemke, R.L., Le, A., and Jackson, J.H. (1999). Four human Ras homologs differ in their abilities to activate Raf-1, induce transformation, and stimulate cell motility. J. Biol. Chem. *274*, 17164–17170.
45. Latinis, K.M., Carr, L.L., Peterson, E.J., Norian, L.A., Eliason, S.L., and Koretzky, G.A. (1997). Regulation of CD95 (Fas) ligand expression by TCR-mediated signaling events. J. Immunol. *158*, 4602–4611.
46. Trent, J.C., II., McConkey, D.J., Loughlin, S.M., Harbison, M.T., Fernandez, A., and Ananthaswamy, H.N. (1996). Ras signaling in tumor necrosis factor-induced apoptosis. EMBO J. *15*, 4497–4505.
47. Ferrari, G., and Greene, L.A. (1994). Proliferative inhibition by dominant-negative Ras rescues naive and neuronally differentiated PC12 cells from apoptotic death. EMBO J. *13*, 5922–5928.
48. Gomez, J. Martinez, C., Fernandez, B., Garcia, A., and Rebollo, A. (1997). Ras activation leads to cell proliferation or apoptotic cell death upon interleukin-2 stimulation or lymphokine deprivation, respectively. Eur. J. Immunol. *27*, 1610–1618.
49. Vos, M.D., Ellis, C.A., Bell, A., Birrer, M.J., and Clark, G.J. (2000). Ras uses the novel tumor suppressor RASSF1 as an effector to mediate apoptosis. J. Biol. Chem. *275*, 35669–35672.
50. Lu, D.C., Rabizadeh, S., Chandra, S., Shayya, R.F., Ellerby, L.M., Ye, X., Salvesen, G.S., Koo, E.H., and Bredesen, D.E. (2000). A second cytotoxic proteolytic peptide derived from amyloid beta-protein precursor. Nat. Med. *6*, 397–404.
51. Sambrook, J., and Russell, D.W. (2001). Molecular Cloning: A Laboratory Manual, Third Edition. (Cold Spring Harbor, NY: Cold Spring Harbor Laboratory Press).
52. van Engeland, M., Ramaekersz, F.C.S., Schutte, B., and Reutelingsperger, C.P.M. (1996). A novel assay to measure loss of plasma membrane asymmetry during apoptosis in adherent cells in culture. Cytometry *24*, 131–139.
53. Boustead, C.M., Brown, R., and Walker, J.H. (1993). Isolation, characterization and localization of annexin V from chicken liver. Biochem. J. *291*, 601–608.

54. Vermes, I., Haanen, C., and Reutelingsperer, C. (2000). Flow cytometry of apoptotic cell death. J. Immunol. Methods *243*, 167–190.
55. Rabizadeh, S., Rabizadeh, S., Ye, X., Wang, J.J., and Bredesen, D.E. (1999). Neurotrophin dependence mediated by p75 NTR: contrast between rescue by BDNF and NGF. Cell Death Differ. *6*, 1222–1227.
56. Sperandio, S., deBelle, I., and Bredesen, D.E. (2000). An alternative, nonapoptotic form of programmed cell death. Proc. Natl. Acad. Sci. USA *97*, 14376–14381.